IEPC-95-118

BEHAVIOUR OF QUASI-STEADY ABLATIVE MPD THRUSTERS WITH DIFFERENT PROPELLANTS[1]

Giorgio PACCANI[2], Ugo CHIAROTTI[3]
Department of Mechanics and Aeronautics, University of Rome "La Sapienza"
Rome, Italy

Abstract

This paper deals with quasi-steady ablative MPD thrusters with instantaneous power of a few megawatts during shots of about one millisecond. A coaxial thruster with radially-positioned bar-shaped propellant was investigated while working with four different polymers acting as propellants [Polytetrafluoroethylene (PTFE,Teflon®), Ethylene-Tetrafluoroethylene resin (ETFE, Hyflon®), Polyethylene (PE) and Ethylene-Chlorotrifluoroethylene resin (ECTFE, Halar®)].

Voltage, current, propellant-ablated mass, jet velocity and impulse bit were measured for five different values of energy per shot in the 1666÷3000 joule range.

The electric parameters show very similar values with all propellants. Generally speaking, Polyethylene (having higher values of bond and ionization specific energy and lower average atomic weight) has a different behaviour compared to the other three, which indeed follow similar trends: apparently, their performances show the typical features of high ionization regimes. PTFE offers the highest thrust and thrust-to-power ratio figures, while ETFE the lowest ones. PE shows the highest exhaust velocity.

NOMENCLATURE

A = propellant surface area
B = magnetic induction field
b = Maecker law coefficient
C = capacity
E, e = energy
e = electron charge
F, f = thrust
i = current
I_b = impulse bit
k = constant
M = molecular/atomic mass
m = ablated mass per shot
N_0 = Avogadro number
P, p = power
Q, q = charge
T = temperature
U, u = energy related to the matter structure
v = velocity
V = electric potential
w = exhaust velocity
Z = impedance
z = level

Greek Symbols

α_i = ionization degree
β_d = dissociation degree
η = efficiency
μ_0 = vacuum magnetic permeability
ν_c = collision frequency
ρ = anode-to-cathode radius ratio
τ = discharge duration
Ω = Hall parameter
ω_B = gyro frequency

Subscripts

0 = initial
c = critic, collision-related
d = dissociation-related
e = equivalent, effective
em = electromagnetic
g = bond
i = ionization-related
j = related to exhaust jet
p = related to propellant vaporization, dissociation and ionization
Q = heat
v = vaporization
t = thruster
tr = transmission

---

(1) This work is sponsored by MURST (*Ministero dell'Universita' e della Ricerca Scientifica e Tecnologica*) and by ASI (*Agenzia Spaziale Italiana*).

(2) Scientist Engineer

(3) Graduate Student

1 - INTRODUCTION

MPD thrusters produce jet acceleration through the exertion of electromagnetic forces on charged particles coming from the ionization of propellants which may initially be in gas, liquid or solid state. The thruster functioning is different in the three cases, i.e. depending on the initial propellant state. In physical terms, the energy exerted on propellants to obtain ionized particles increases shifting from the first to the third case. In particular, with solid propellants, the particles available for acceleration are those the electric arc subtracts to the solid lattice through an ablation process. Hence, in functional terms - unlike what happens in the first two cases - the propellant mass-flow rate available for acceleration is no externally-controllable variable: it is therefore an "intrinsic" parameter. It is determined by the arc and propellant characteristics and by the arc-propellant interaction [18]. The whole functioning is thus conditioned by the ablation process and in particular by the propellant chemical-physical features which influence that process.

In the past, studies on ablative MPD thrusters adopting different propellants were carried out on PPT micro thrusters [4]. In the framework of a general survey on solid-propelled quasi-steady ablative MPD thrusters with instantaneous power of a few megawatts, a comparative experimental analysis was conducted on the functioning of this kind of systems with different propellants.

1.1 - THE ABLATION PROCESS

According to different studies, in phenomenological terms, a solid ablation process is influenced by different parameters such as ion and electron energy, plasma density, heat flux, ion current density on the surface and pressure [7,8,12,15,16].

Whenever the energy density is small, it exerts a uniformly-distributed action on the solid surface, which gives rise to a thermal process leading to vaporization or sublimation ("*thermally activated process*"). Whenever the energy density is higher, different kinds of forces emerge and act on the single solid particles thus causing their subtraction to the crystal lattice ("*physical sputtering*").

However, in the whole energy range, chemistry plays a fundamental role. The presence of particularly reactive atoms in the plasma heavily contributes to the atom subtraction from the solid surface through an essentially three-phased process: solid adsorption of appropriate chemical species, formation of reaction products and desorption of such products.

Finally, the etching phenomenon is amplified by the presence of ionized particles ("*ion-enhanced gas-surface chemistry*") following different mechanisms according to the chemical system within which one operates [8] ("*chemically enhanced physical sputtering*", "*chemical sputtering*", "*damage-induced chemical reaction*" etc....).

1.1.1 - PROPELLANT ABLATION IN MPD THRUSTERS

Consider now the propellant ablation in quasi-steady MPD thrusters during the shot stationary phase. In the discharge chamber, average electron temperature is at most of several electron-volt, while electron density is comprised in a very wide range ($10^{21} \div 10^{27}$ m^{-3}) [3, 13, 20].

According to some Authors [13, 17, 20], propellant ablation in these conditions may be described as a thermal phenomenon caused by arc-emitted radiations; assuming arc as a black body, a direct relation is obtained between the emission spectrum and its temperature [17]. Only a small portion of the radiation emitted reaches

the propellant surface. Most of them are absorbed by a superficial vapor layer having a considerably lower temperature than the arc [17]. The propellant sublimates, thus giving rise to particles penetrating the vapor layer first and the arc later, where they dissociate and ionize. This introduction of new matter in the plasma causes a contemporaneous pressure increase and cooling. However, the plasma tends to warm up owing to the current flow; at the same time, the arc outward radiation and the mass loss towards the nozzle subtract energy and lead to the plasma cooling.

On the basis of the plasma temperatures and assuming the propellant is surrounded by its vapor coating having an insulating effect from plasma, a physical sputtering is excluded and ablation is to be attributed to a thermal phenomenon possibly along a side with chemical reactions due the presence of chemically hyper-reactive ions (such as F, for example).

Inevitably, any process taking place in the arc is controlled by the propellant ablation, which in turn is controlled by the radiation flow coming from the arc itself.

1.2 - THE ENERGY SCHEME

In energy terms a thruster functioning schematization may be based on the fundamental parameter E_t that is the energy the thruster utilizes in one shot, i.e. the energy used in the electric arc. The radiative energy the arc emits is shared among the different processes taking place in the discharge chamber. Part of the energy (E_p) goes in the process of generating an ionized gas from a solid substance and providing the particles for acceleration; part of it (E_Q) reaches the thruster walls and heats them up and part of it (E_a) reaches the ionized particles and causes their acceleration, thus giving rise to the jet acceleration; hence:

$$E_t = E_p + E_Q - E_j = m e_p + E_Q + E_j \qquad (1.1)$$

where the specific energy, e_p, depends on the propellant used.

The ionized-gas generation process, employing the E_p energy, may in turn be summarized as follows. The solid propellant molecules thermalize and vaporize (or sublimate) (*pyrolysis*). The vacuum thermal pyrolysis may produce different substances, according to the conditions where it develops. The relatively cold gas produced, coming into contact with the arc plasma, is subject to further dissociation and ionization processes. In each of them the gas adsorbs energy, namely vaporization energy (E_v), dissociation energy (E_d) and ionization energy (E_i) respectively, as

$$E_p = E_v + E_d + E_i \quad \Rightarrow \quad e_p = e_v + \beta_d e_d + \alpha_i e_i \qquad (1.2)$$

where α_i and β_d are respectively the ionization and the dissociation degree while the specific energies e_v, e_d and e_i are in turn propellant characteristics.

2 - SOLID PROPELLANT CHARACTERISTICS

Examine now the main thrust characteristics of a solid propellant relative to the thruster functioning. On the basis of the previous schematization, the energy poured in the jet acceleration (E_j) - with other quantities

remaining equal - increases as the energy flown in the ionized-gas generation process (E_p) decreases. The parameter having the main impact on this last process is the one relative to ionization: primary characteristic for the selection of a solid propellant is therefore a low ionization potential in its atoms or molecules. Indeed, in the past, propellants consisting of a base substance with addition of substances with low extraction potential were used - notably alkaline and alkaline-earth metals inserted in polymers - but no substantial progress was obtained [4]. Low values of vaporization and of dissociation energies are therefore preferred; materials with low sublimation temperature, such as some iodine compounds or some plastic materials, are then appropriate.

Past experiments have shown that a heavier molecular weight in the accelerated gas implies [9,11]: higher thrust-to-power ratio (the thrust provided by molecular gases is usually greater than that produced by monatomic gases) and lower exhaust velocity. However, experimental data are not always smoothly connectable to the commonly accepted theories.

The thrust ($F = \dot{m}\, w$) depends on the mass-flow rate and on velocity; both depending on the mass of accelerated particles. A priori, only in qualitative terms one might state that an increase in the particle mass implies a rise in the mass-flow rate and a fall in velocity.

The particle mass influences the Hall parameter

$$\Omega = \frac{\omega_B}{\nu_c} = \frac{1}{m}\frac{q\,B}{\nu_c}; \qquad (2.1)$$

which affects the particles paths in electromagnetic fields: generally speaking, its impact incidence cannot be computed *a priori*.

In chemical terms, solid propellants should contain elements which, once transformed into gas, strongly react with their own surface. Hence, fluropolymers would bring advantages [19], as they release fluorine, an extremely reactive substance. Experimental analyzes have shown that, with equal energy adsorption, even light modifications in plasma composition, with the addition of suitable elements, might lead to a remarkable rise in the ablated mass [16].

In electrical terms, the propellant should consist of an insulating material; however, some ablative substances have the peculiarity of forming a conductive coat on their surfaces. There are Authors who think that this inhibits the ablation process [4, 5]. Furthermore, when the propellant comes into contact with both electrodes - as happens in breech-fed thrusters -, a misfunctioning might emerge with consequent current loss [5]. Besides, some plastics - ETFE [4], for instance - may show a charring phenomenon, notably polymers subject to strong thermal shocks change their physical structures to form carbonized areas, probably owing to partial fusion, which make the propellant no longer usable.

Some plastic polymers show a whole set of characteristics which are not simultaneously available in inorganic materials and which make them most suitable to act as propellants. They can be easily sublimated within a wide range of temperature and pressure values; indeed, they possess good mechanical properties and high electrical resistivity. Furthermore, the gas generated by sublimation can be easily ionized. When utilized in pulsed plasma thrusters, such polymers have provided the best performances, particularly PTFE [4]. The following four materials were thus chosen for the experimental analysis: Polytetrafluoroethylene (PTFE) [$(C_2F_4)_n$, Teflon®)], Ethylene-Tetrafluoroethylene resin (ETFE), [$(C_2H_4 - C_2F_4)_n$, Hyflon®, Tefzel®)]. Polyethylene (PE) [$(C_2H_4)_n$]. Ethylene-Chlorotrifluoroethylene resin (ECTFE) [$(ClC_2F_3 - C_2H_4)_n$, Halar®].

3 - EXPERIMENTAL APPARATUS AND OPERATIVE MODALITIES

The propulsive system used in the experimental analysis was made of a pulse-forming network with a total capacity of 0.072 F comprising two 15-capacitor branches and of a coaxial thruster with radially-positioned bar-shaped propellant (Fig.3.1). The discharge is triggered with an 0÷20 kV device.

The following quantities were measured: the instantaneous electric parameters (anode-to-cathode potential difference [V(t)] and discharge current intensity [i(t)]), the ablated mass per shot (m), the impulse bit (I_b) and the jet exhaust velocity (w).

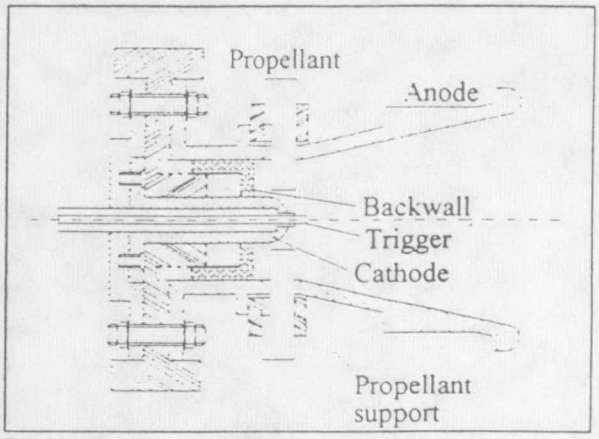

Fig. 3.1 -

The electrode potential was directly measured through an oscilloscope, while the current was detected by a Rogowsky-probe-based device. The average value taken over 30 measurements was assumed as the standard value for each electric parameter. The ablated mass was obtained weighting the propellant before and after single shot series by means of an electronic balance with a ±1 mg accuracy. The minimum shot number of each series was chosen so as to enable the ablated mass to exceed 50 mg in each series.

The impulse bit value was taken as the average figure among 5 measurements (Fig. 3.2) obtained analyzing the pendulum motion produced by a shot of the thruster mounted on the pendulum itself (Fig. 3.3). The impulse bit is given by [22]

$$I_b = m A \omega \qquad (3.1)$$

where m is the equivalent pendulum mass, A the oscillation amplitude (Fig. 3.3) and ω its pulsation. These last two were measured through a computerized elaboration of a signal provided by an 0.001-mm-resolution proximeter.

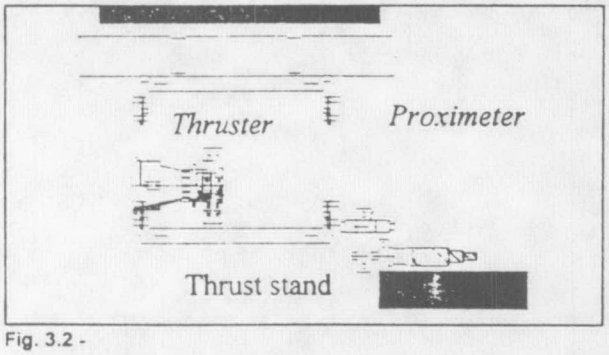

Fig. 3.2 -

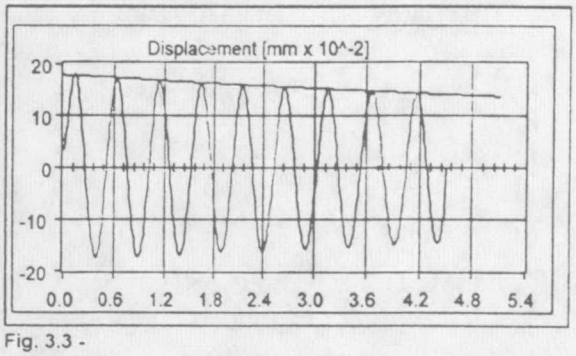

Fig. 3.3 -

Finally, velocity was taken as the average value among 30 measurements determined with the time-of-flight method through cross-correlations of the signals emitted by two double Langmuir probes acting as targets [23].

A computer elaboration of the values obtained has led to the following parameters:

$$E_t = \int_0^{\infty} i(t) \cdot V(t)\,dt \qquad (3.2) \qquad Q = \int_0^{\infty} i\,dt \qquad (3.3)$$

$$\Psi = \int_0^{\infty} i^2(t)\,dt \qquad (3.4) \qquad \int_0^{\tau_e} i^2\,dt = 0.98\,\Psi \Rightarrow \tau_e \qquad (3.5)$$

$$i_e = \left(\frac{\Psi}{\tau_e}\right)^{\frac{1}{2}} \qquad (3.6) \qquad Z_e = \frac{E_t}{\Psi} \qquad (3.7) \qquad V_e = Z_e \cdot i_e. \qquad (3.8)$$

Each measurement was taken for different levels of PFN stored energy

$$E_0 = \frac{1}{2} C V_0^2 \qquad (3.9)$$

obtained setting the initial voltage value (V_0). The measurements were chosen in correspondence to the values of E_0 in the 1666÷3000 J range at intervals of 333 J in an 0.5 m^3 vacuum chamber with a back-pressure of $(7.5\pm2.5)*10^{-3}$ Pa.

To compare the propellant performances. the value of some of the propellant properties was computed following a homogenous procedure. Indeed, for simplicity reasons, the chemical bond values of the materials [2] were assumed as values of the propellant vaporization and dissociation energies. The gas ionization energy was computed as the sum of the ionization energies of the single dissociated elements [6, 24]. It was obtained respectively:

- Polytetrafluoroethylene (PTFE) [$(C_2F_4)_n$, Teflon®), M_a=16.67 g/mole, U_i/N_0 =15.77 eV/atom, u_i=91 MJ/kg, u_g=24.7 MJ/kg].
- Ethylene-Tetrafluoroethylene resin (ETFE), [$(C_2H_4 - C_2F_4)_n$, Hyflon®, Tefzel®), M_a=10.67 g/mole, U_i/N_0 =14.28 eV/atom, u_i=129 MJ/kg, u_g=37.7 MJ/kg],
- Polyethylene (PE) [$(C_2H_4)_n$, M_a=4.67 g/mole, U_i/N_0 =12.79 eV/atom, u_i=264 MJ/kg, u_g=87.1 MJ/kg].
- Ethylene-Chlorotrifluoroethylene resin (ECTFE) [$(Cl\,C_2F_3 - C_2H_4)_n$, Halar®, M_a=12.08 g/mole, U_i/N_0 =13.86 eV/atom, u_i=111 MJ/kg, u_g=32.6 MJ/kg).

4 - EXPERIMENTAL RESULTS

4.0.1 - ELECTRICAL PARAMETERS

The electrical transmission efficiency

$$\eta_{tr} = \frac{E_t}{E_0} \qquad (4.1)$$

is slightly decreasing with energy, but always comprised in the 0.45÷0.50 range.

The characteristic curve V-i is almost linearly increasing (Fig. 4.1), impedance following a trend only slightly decreasing with energy (Fig.4.2). This last is marginally higher for ETFE. The values are in the 8.5÷12 mΩ range.

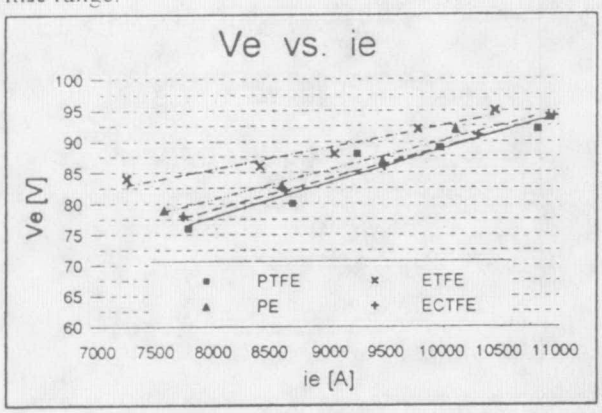

Fig. 4.1 -

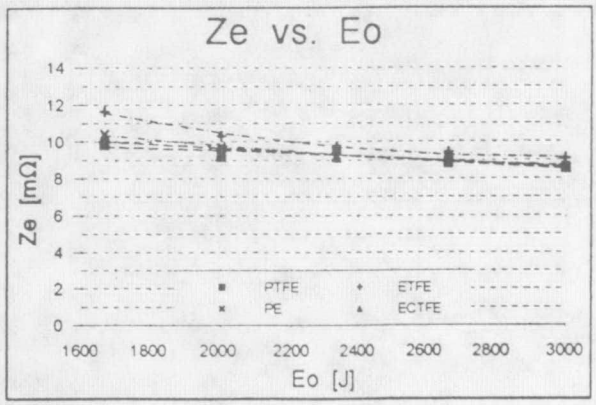

Fig. 4.2 -

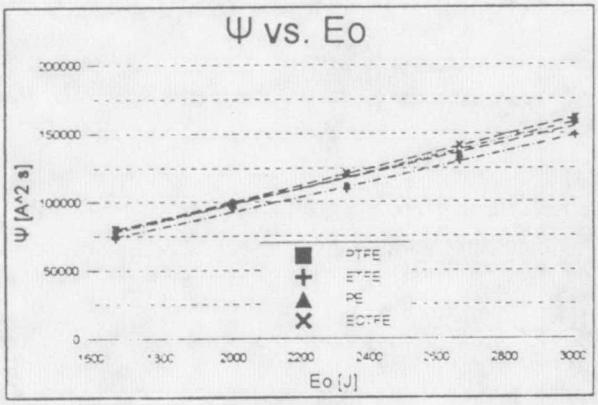

Fig. 4.3 -

Parameter Ψ shows the typical linear trend increasing with energy. The trends obtained with different propellants show common values except for the one relative to ETFE, which is slightly lower (Fig.4.3).

When using ETFE - some bars coming into contact with both electrodes - the conductive coat phenomenon emerged. A superficial propellant carbonization was noted, with accidental spontaneous sparkling due to anode-to-cathode potential differences of about 100 V. The phenomenon finds its explanation in what follows. After a given number of (regular) shots, the conductive coat is formed. When the propellant is put into contact with both electrodes, it is continuously crossed by current, which heats it up and makes it vapor and trigger the discharge. In the long distance, this leads to carbonization. The phenomenon doesn't happen whenever the bars are no longer in simultaneous contact with both electrodes.

The equivalent shot duration (3.5) proves constant with energy and similar for all propellants ($\tau_e \approx 1.35$ ms).

4.0.2 - ABLATED MASS

The ablated mass (m) is always almost linearly increasing with energy E_t (Fig. 4.4) and the Ψ parameter (Fig. 4.5); with equal energy or Ψ

$$m(PTFE) > m(PE) > m(ECTFE) \geq m(ETFE) \qquad (4.2)$$

is obtained in each case.

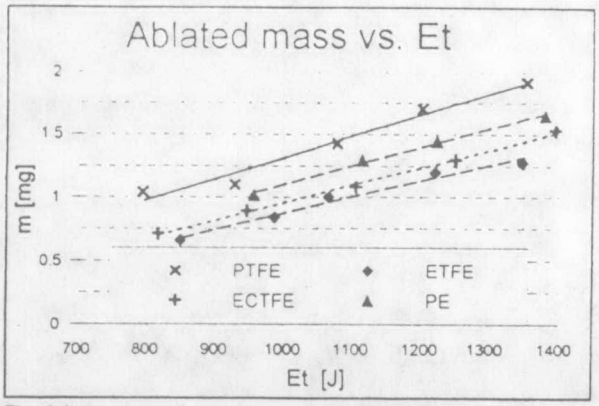

Fig. 4.4 -

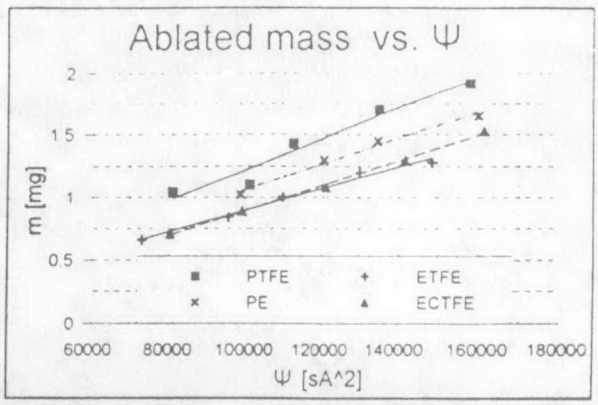

Fig. 4.5 -

Assuming

$$E_p = m(e_v + \beta_d e_d + \alpha_i e_i) = k_p E_t, \tag{4.3}$$

the ablated mass becomes

$$m = \frac{k_p E_t}{e_v + \beta_d e_d + \alpha_i e_i}. \tag{4.4}$$

Generally speaking, it is difficult to compute the ionization degree. However, assuming the same average ionization level for all existing species ($z_i = q_i/e$ = cost). a rough indicator with relative value may be identified according to the computable quantities [transferred charge (Q) and mass (m) per shot]

$$\alpha_i = \frac{Q}{q_i N} = \frac{Q M}{q_i z_d m N_0}, \tag{4.5}$$

N being the number of ablated particles; with equal ionization level, this parameter follows a trend decreasing with energy. In particular, the charge-to-mass ratio (Q/m) changes with the current inverse as charge modifies with current while mass (Fig. 4.4) changes with squared current.

The k_p parameter depends on the propellant used, as it considers the propellant area exposed to the arc radiations and the radiation transparency of vapor near the propellant. The former only changes whenever the arc geometry modifies, while the latter is different for different propellants and can considerably affect the energy quantity reaching the radiation-exposed propellant walls.

On the basis of the previous expression, a full ionization is inferred for PTFE, ETFE and ECTFE and a half ionization (or less) for PE. Hence (4.4), assuming a full dissociation (β_d=1). k_p(PTFE)≈k_p(ETFE)≈k_p(ECTFE)≈0.14÷0.17 and k_p(PE)≈0.20÷0.23 respectively. The higher vapor (containing Hydrogen) reactivity and/or transparency may account for the higher value of k_p(PE).

Coming back to the experimental results, with regard to the first three propellants named, the ablated mass increases as binding energy (i.e. e_v+e_d) decreases, the ionization energy-related term showing similar values in all cases. With regard to PE, its ablated mass is greater owing to a higher value of its k_p.

4.0.3 - VELOCITY

When energy changes, velocity keeps almost constant for all propellants, though it reveals - as shown in previous studies - a slightly increasing trend (Fig. 4.6). Besides, with equal E_t

$$w(PE) > w(ECTFE) > w(ETFE) > w(PTFE); \tag{4.6}$$

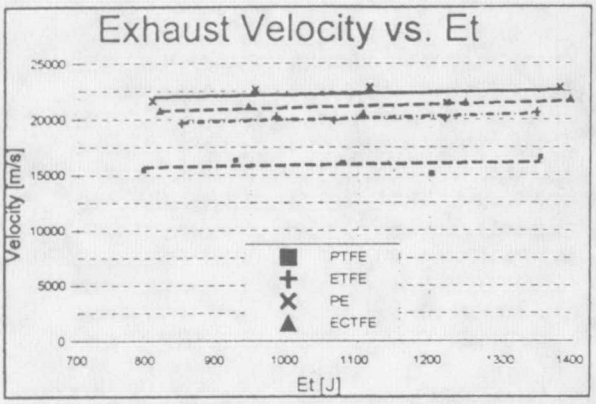

Fig. 4.6 -

propellants with lower atomic weights produce higher velocity values, with the exception of ECTFE and ETFE, whose atomic weights, however slightly differ one from the other.

4.0.4 - IMPULSE BIT AND THRUST

During a shot, a quasi-steady thruster functioning closely resembles a steady thruster functioning operating with current equal to the "effective" one as defined before (3.6). The equivalent shot time (3.5) being almost constant, all comments relative to the (measured) impulse bit also apply to thrust ($F = I_b/\tau_e$); the impulse bit follows a trend increasing with the discharge energy (E_t) (Fig.4.7) with a lower PE slope and the following value scale

$$I_b(PTFE) > I_b(ECTFE) > I_b(PE) \geq I_b(ETFE). \tag{4.7}$$

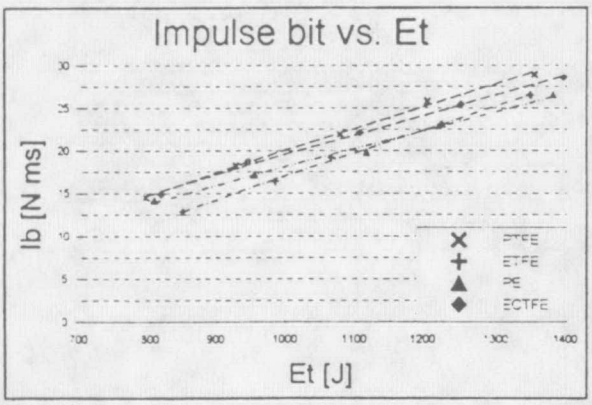

Fig. 4.7 -

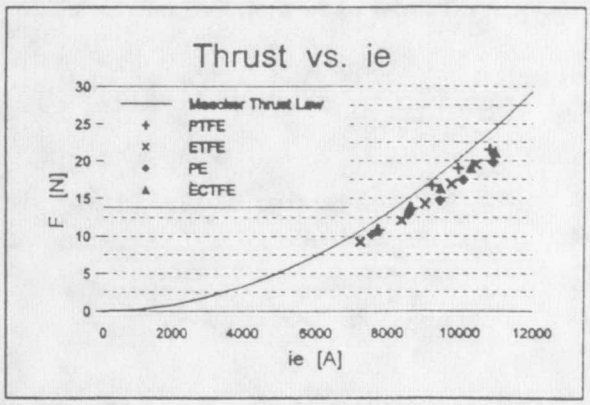

Fig. 4.8 -

Its trend follows the Maecker law (Fig. 4.9):

$$F_{em} = b\, i^2 \tag{4.8}$$

being

$$b = \frac{\mu_0}{4\pi}\left[\ln \rho + \frac{3}{4}\right] \tag{4.9}$$

where ρ is the anode-to-cathode radius ratio; being anode conically shaped, the cone radius average value was assumed as anode radius. The Maecker law, however, lead to higher values than the experimental ones; it might depend on the assumed value of the b parameter. Notice that, in the Maecker law, the anode radius conceptually represents the average radius as against the current axial distribution along the anode. Its value is lower than the one assumed, as discharge tends to concentrate on the initial tract, where the radius is shorter.

The thrust, computed as the mass-flow rate times the exhaust velocity, attains higher values than those obtained through its direct measurement, though the figures are very similar, except for PE (Figs. 4.9, 4.10); all of which may confirm the previous remarks on ionization degree; indeed, the measured velocity is the ion velocity and, if these do not form the whole mass, the remaining nonionized part has lower exhaust velocity.

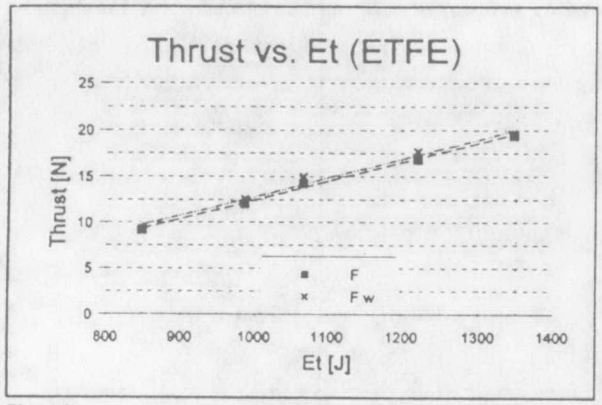

Fig. 4.9 -

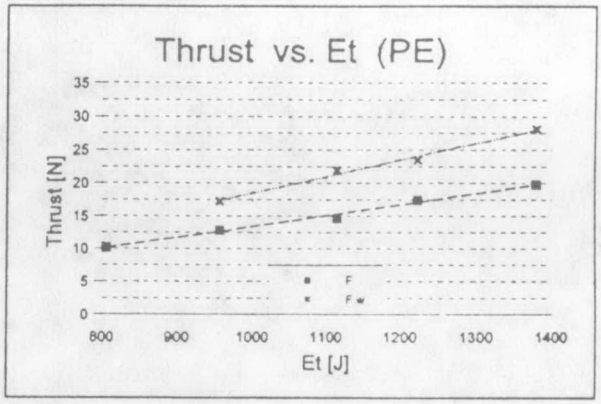

Fig. 4.10 -

The thrust-to-power ratio has an almost linear increasing trend with E_t for all propellants but with a different slope for each of them; everywhere the PTFE shows the highest values (Fig. 4.11).

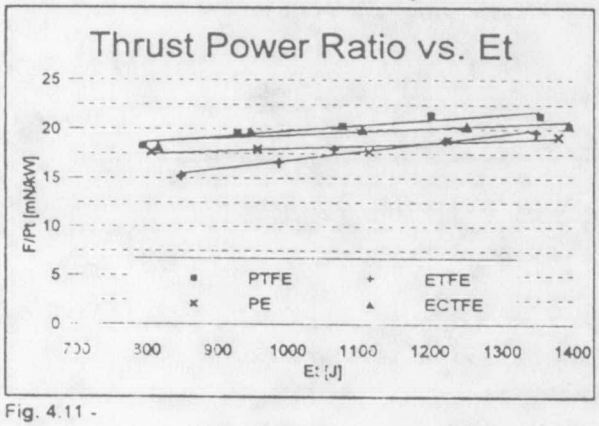

Fig. 4.11 -

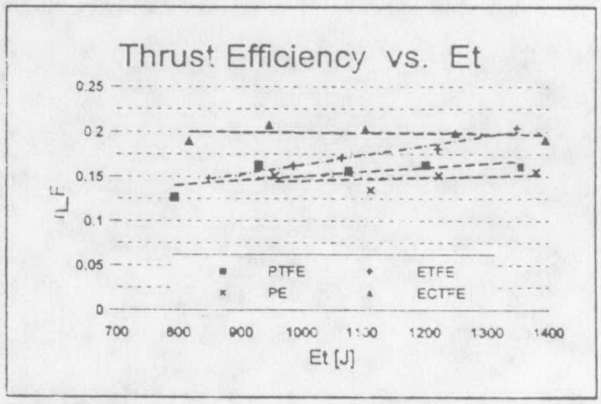

Fig. 4.12 -

4.0.5 - THRUST EFFICIENCY

Finally, thrust efficiency

$$\eta_F = \frac{E_J}{E_t} = \frac{I_b^2}{2\,\dot{m}\,E_t} \qquad (4.10)$$

shows a trend almost consistent with the one of shot energy for all propellants except for ETFE, when it shows an increasing trend, being in correspondence to higher energies (Fig. 4.12)

$$\eta_F(ECTFE) \approx \eta_F(ETFE) > \eta_F(PTFE) > \eta_F(PE) \tag{4.11}$$

4.1 - REMARKS

Some phenomena taking place in MPD thrusters have been correlated [10, 14] to the Alfvèn velocity [1]

$$v_c = \sqrt{\frac{2\,e\,V_i}{M}} \tag{4.12}$$

and to the critical ionization current, corresponding to the full ionization regime [21]

$$i_c = \left(\frac{2\,E\,V_i\,\dot{m}}{M\,b}\right)^{1/2} = \left(\frac{\dot{m}}{b}\right)^{1/2} v_c \tag{4.13}$$

These quantities have a strict physical meaning if measured for single species of propellant-forming particles, each characterized by its own molecular weight. The following remarks are based on the following rough assumption: the molecular weight is computed as the mean molecular weight of propellants considered as completely dissociated matters.

The propellants, which were estimated as full ionized, show mean velocities higher than the respective Alfvèn velocities (v_c), while PE, estimated as half ionized, shows a velocity very close to the respective Alfvèn one (Tab. 4.i). This results agree with the Block-Fahleson experiment [1].

Tab. 4.i -

	PTFE	ETFE	PE	ECTFE
w [m/s]	15917	20116	22311	21215
v_c [m/s]	13511	16070	22989	14904

As for ablative thrusters, equal thrusters with different propellants have, with equal current, different mass-flow rates. Then for a comparison to be drawn, the specific thrust is to be considered (Fig. 4.13)

$$f = \frac{F_{em}}{\dot{m}} \equiv w = b\,\frac{i_e^2}{\dot{m}} = b\,\hat{i}_e^2 \tag{4.14}$$

where a *specific current*

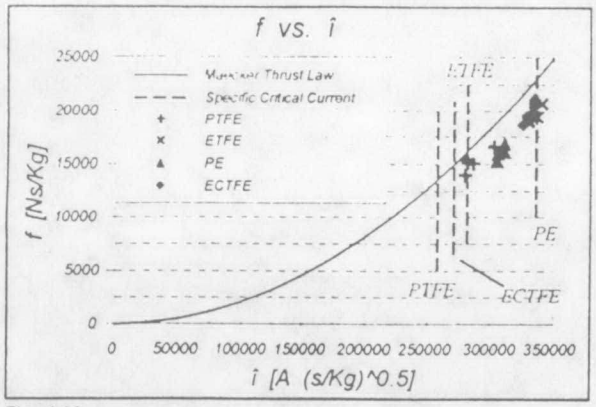

Fig. 4.13 -

$$\hat{i}_c = \sqrt{\frac{i_c^2}{\dot{m}}} = \sqrt{\frac{\psi}{m}} \qquad (4.15)$$

has been introduced. This is a constant (Fig. 4.5) characteristic of each propellant [24]. Introducing then a *specific critical current*

$$\hat{i}_{ec} = \frac{i_{ec}}{\sqrt{\dot{m}}} = \left(\frac{2\,e\,V_i}{M\,b}\right) = \left(\frac{v_c}{b}\right)^{1/2} \qquad (4.16)$$

the specific current experimental values are all greater than the critical ones, but for PE, which shows lower values (Fig. 4.13).

To conclude with, four plastic polymers were tested as propellants in a quasi-steady coaxial solid-propellant ablative MPD thruster. Apparently PTFE, ETFE and ECTFE - unlike PE - have similar behaviours showing the typical features of high ionization regimes. Indeed the thrust performance of the four propellants is rather homogeneous; notably a slightly higher thrust and thrust-to-power ratio were obtained for PTFE and a higher thrust efficiency for ECTFE and ETFE.

REFERENCES

[1] **Alfvén H.**: *"Collision Between a Non-Ionized Gas and a Magnetized Plasma"*; Reviews of Modern Physics, Vol. 32, No. 4, Oct.1960, pp. 710-713.

[2] **Pauling L.**:*The Nature of the Chemical Bond*; New York, Cornell University Press, 1965.

[3] **Vondra R., Thomassen K. and Solbes A.**: *"A Pulsed Electric Thruster for Satellite Control"*, Proceedings of the IEEE, Vol. 59, No. 2, Feb. 1971.

[4] **Palumbo D. J., et al.**: *"Pulsed Plasma Propulsion Technology"*, Report AFRPL-TR-73-79, Air Force Rocket Propulsion Laboratory, Sept. 1973.

[5] **Liebing L. and Seidel F.**: *"A Low Current Pulsed Ablation Plasma Thruster"*, AIAA Paper 73-1068, AIAA 10th Electric Propulsion Conference, Lake Tahoe, Nevada, Oct-Nov.1973.

[6] **Silvestroni P.**: *Fondamenti di Chimica*; Roma, Veschi Editore, 1976.

[7] **Sovey J. S.**: *"Ion Beam Sputtering of Fluoropolymers"*, J.Vac. Sci. Technol., Vol.16, No.2, Mar-Apr. 1979, pp. 813-816.

[8] **Winters H. F., Coburn J. W. and Chuang T.J.**: *"Surface Process in Plasma-Assisted Etching Environments"*, J.Vac. Sci. Technol. B , Vol.1, No.2, Apr-June 1983, pp. 469-480.

[9] **Uematsu K., Morimoto S. and Kuriki K.**; *"MPD Thruster Performance with Various Propellants"*: Journal of Spacecraft and Rockets, Vol. 22, No. 4, July-Aug. 1985, pp. 412-416.

[10] **Choueiri E.Y., Kelly A.J. and Jahn R.G.**: *"The Manifestation of Alfvén's Hypothesis of Critical Ionization Velocity in the Performance of MPD Thrusters"*, AIAA 85-2037, AIAA/DGLR/JSASS 18th International Electric Propulsion Conference, Alexandria, Virginia, Sept-Oct. 1985.

[11] **Bühler R. D.**: *"Plasma Thruster Development: Magnetoplasmadynamic Propulsion, Status and Basic Problems"*, Report AFRPL-TR-86-013, Air Force Rocket Propulsion Laboratory, Feb.1986.

[12] **Steinbrüchel Ch., Curtis B. J., Lehmann H. W. and Widmer R.**: *"Summary Abstract: Diagnostics of Low-Pressure Oxygen Radio-Frequency Plasmas and the Mechanism for Polymer Etching: A Comparison of Reactive Sputter Etching and Magnetron Sputter Etching"*, J.Vac. Sci. Technol. A , Vol.4, No.3, May-June 1986, pp. 1798-1799.

[13] **Ruchti C. B. and Niemeyer L.** : *"Ablation Controlled Arcs"*, IEEE Trans. Plasma Sci., Vol. PS-14, No 4, Aug. 1986, pp. 423-434.

[14] **Turchi P.J.**:*"Critical Speed and Voltage-Current Characteristics in Self-Field Plasma Thrusters"*; J. Propulsion, Vol. 2, No. 5, Sept-Oct. 1986, pp.398-401.

[15] **Hofer W. O.**: *"Plasma Surface Interactions: The Role of Charged Particle Emission"*, J.Vac. Sci. Technol. A, Vol.5, No.4, July-Aug. 1987, pp. 2213-2216.

[16] **D'Agostino R.** (ed.): *Plasma Deposition, Treatment, and Etching of Polymers*; San Diego, Academic Press Inc. 1990.

[17] **Gilligan J. G. and Mohanti R. B.**: *"Time-Dependent Numerical Simulation of Ablation-Controlled Arcs"*, IEEE Trans. Plasma Sci., Vol. 18, No. 2, Apr. 1990, pp. 190-197.

[18] **Paccani G.**: *"Non-Steady Solid Propellant MPD Thruster Experimental Analysis Concepts"*; AIAA-90-2674, AIAA/DGLR/JSASS 21st International Electric Propulsion Conference, Orlando, FL, July 1990.

[19] **Myers R. M.**: *"Electromagnetic Propulsion for Spacecraft"*, AIAA 93-1086, AIAA/AHS/ASEE Aerospace Design Conference, Irvine, CA, Feb.1993.

[20] **Bourham M. A., Gilligan J. G. and Hankins O. E.**: *"Plasma Material Interaction in Electrothermal and Electromagnetic Launchers"*, AIAA-93-3172, AIAA 24th Plasmadynamic & Lasers Conference, Orlando, FL, July 1993.

[21] **Choueiri E.Y.**:*"Plasma Physics of the MPD Thruster"*, private communication.

[22] **Paccani G. and Ravignani R.**:*"Sistemi di misura della spinta di propulsori MPD"*, Aerotecnica Missili e Spazio, Jan-June 1994.

[23] **Paccani G. and Di Zenzo S.**:*"MPD Thrusters Computer-Operated Jet Velocity Measurement"*, forthcoming.

[24] **Paccani G.**: *"Studi sui meccanismi fisici di base nei propulsori MPD"*; ASI, Rapporto Finale, 1995.

Acknowledgments

The Authors would like to thank Ausimont C.R.S. for providing the Hyflon® and Halar® propellants.